*Journal of General Virology* (2005), **86**, 3081–3090 DOI 10.1099/vir.0.81158-0

# Antiviral activity of morpholino oligomers designed to block various aspects of *Equine arteritis virus* amplification in cell culture

Erwin van den Born,[1] David A. Stein,[2] Patrick L. Iversen[2] and Eric J. Snijder[1]

[1]Molecular Virology Laboratory, Department of Medical Microbiology, Center of Infectious Diseases, Leiden University Medical Center, LUMC P4-26, PO Box 9600, 2300 RC Leiden, The Netherlands

[2]AVI BioPharma Inc., 4575 SW Research Way, Corvallis, OR 97333, USA

Correspondence
Eric J. Snijder
e.j.snijder@lumc.nl

Received 1 May 2005
Accepted 22 July 2005

The antiviral efficacy of ten antisense phosphorodiamidate morpholino oligomers (PMOs) directed against *Equine arteritis virus* (EAV), a nidovirus belonging to the family *Arteriviridae*, was evaluated in mammalian (Vero-E6) cells. Peptide-conjugated PMOs (P-PMOs) supplied in cell culture medium at micromolar concentrations were efficiently taken up by Vero-E6 cells and were minimally cytotoxic. The P-PMOs were designed to base pair to RNA sequences involved in different aspects of EAV amplification: genome replication, subgenomic mRNA synthesis, and translation of genome and subgenomic mRNAs. A novel recombinant EAV, expressing green fluorescent protein as part of its replicase polyproteins, was used to facilitate drug screening. A moderate reduction of EAV amplification was observed with relatively high concentrations of P-PMOs designed to anneal to the 3′-terminal regions of the viral genome or antigenome. To determine if the synthesis of subgenomic mRNAs could be specifically reduced, transcription-regulating sequences essential for their production, but not for the production of genomic RNA, were targeted, but these P-PMOs were found to be ineffective at transcription interference. In contrast, all four P-PMOs designed to base pair with targets in the genomic 5′ untranslated region markedly reduced virus amplification in a sequence-specific and dose-responsive manner. At concentrations in the low micromolar range, some of the P-PMOs tested completely inhibited virus amplification. *In vitro* translation assays showed that these P-PMOs were potent inhibitors of translation. The data suggest that these compounds could be useful as reagents for exploring the molecular mechanics of nidovirus translation and have anti-EAV potential at relatively low concentrations.

## INTRODUCTION

In recent years, phosphorodiamidate morpholino oligomers (PMOs) have been used as a loss-of-function tool to inhibit gene expression and have provided a useful method to study gene function, especially in the area of developmental biology (Heasman, 2002; Liu *et al.*, 2003; Boguslavsky *et al.*, 2003; Muto *et al.*, 2004). PMOs are single-stranded DNA-mimics, typically synthesized to 20–25 bases in length, and display high biological stability and low toxicity. Most of the PMOs reported to effectively reduce gene expression targeted the 5′ untranslated region (5′ UTR) of mRNA or the first 25 nt 3′ of the translation initiation codon (Summerton, 1999; Heasman, 2002). In instances of translation inhibition, it is presumed that the oligomers form a complex with their mRNA target that physically blocks critical events in pre-initiation, ribosomal scanning or initiation at the start site region. The documented success at translation inhibition has raised the prospect of evaluating the potential of PMOs to block the amplification of viruses, in particular positive-stranded RNA viruses whose replication cycle depends on translation of incoming genomic RNA. For example, PMOs targeted to the hepatitis C virus (HCV) internal ribosome entry site (IRES) were shown to reduce translation of HCV RNA both *in vitro* and *in vivo* (Jubin *et al.*, 2000; McCaffrey *et al.*, 2003). Highly efficient uptake of these uncharged oligomers by cultured cells can be achieved by conjugating PMO to any of a number of arginine-rich peptides (Moulton *et al.*, 2003, 2004). Peptide-conjugated PMOs (P-PMOs) have been demonstrated to have sequence-specific inhibitory effects on the amplification of a coronavirus (Neuman *et al.*, 2004) and several flaviviruses (Kinney *et al.*, 2005; Deas *et al.*, 2005) in cell culture.

In this report, we describe the evaluation of the efficacy of P-PMOs designed to inhibit the amplification of *Equine arteritis virus* (EAV), the prototype of the family *Arteriviridae*, which is united with the families *Coronaviridae* and *Roniviridae* in the order Nidovirales (Snijder & Meulenberg, 2001; González *et al.*, 2003). In addition to the full-length RNA genome (Fig. 1a), EAV and other nidoviruses produce a set of nested subgenomic (sg) mRNAs in infected cells. In the case of arteriviruses and coronaviruses, these sg mRNAs contain a common leader sequence, derived from the 5′-terminal region of the genome, that is fused to different but overlapping 'body sequences', which are derived from the 3′-proximal region of the genome. Thus, sg mRNAs are both 5′- and 3′-coterminal with the genomic RNA. Conserved transcription-regulating sequences (TRSs) precede every open reading frame in the 3′-proximal quarter of the genome (body TRSs) and an additional copy is found at the 3′ end of the leader (leader TRS). Base pairing between the leader TRS (in the plus strand) and body TRS complements in the minus-strand was found to play a critical role in joining the leader and body segments of sg RNAs in arteriviruses and coronaviruses (Pasternak *et al.*, 2001, 2003; Zuniga *et al.*, 2004). The fusion of the sg RNA body to the leader sequence has been postulated to involve discontinuous extension during minus-strand RNA synthesis (Fig. 1b) (Sawicki & Sawicki, 1995). After attenuation of RNA synthesis at the body TRS, the nascent minus-strand is thought to translocate to the 5′-proximal region of the genomic template. Following TRS-guided base pairing with the template, RNA synthesis is resumed, adding the complement of the genomic leader sequence, thus completing the sg minus-strand. Positive-strand sg mRNAs are then transcribed from corresponding minus-strand sg RNA templates (Sawicki & Sawicki, 1995).

The arterivirus genome, and presumably all sg mRNAs, are capped and polyadenylated. It is most likely that translation initiation of the EAV mRNAs is cap-dependent and the ribosomal pre-initiation complex scans the 5′ UTR in a linear manner to identify the translation initiation codon of the replicase gene (van den Born *et al.*, 2005). The viral RNA elements involved in EAV genome replication are poorly defined, but data from our previous studies suggest that at least the 5′-proximal 290 and the 3′-proximal 354 nt are required for efficient replication (Molenkamp *et al.*, 2000b, c; Tijms *et al.*, 2001; van den Born *et al.*, 2005).

Ten P-PMOs were designed to bind specifically to RNA sequences involved in different aspects of EAV amplification: genome replication, sg mRNA synthesis, and translation of genome and sg mRNAs. The 3′-terminal regions of the genome and antigenome were chosen as P-PMO target sites in an attempt to block replication, but only a moderate reduction of virus amplification was observed at relatively high oligomer concentrations. To assess whether the synthesis of sg mRNAs could be blocked exclusively, TRS motifs were targeted, but these P-PMOs were found to be ineffective at interfering with transcription. In contrast, all four of the antisense P-PMOs designed to base pair with

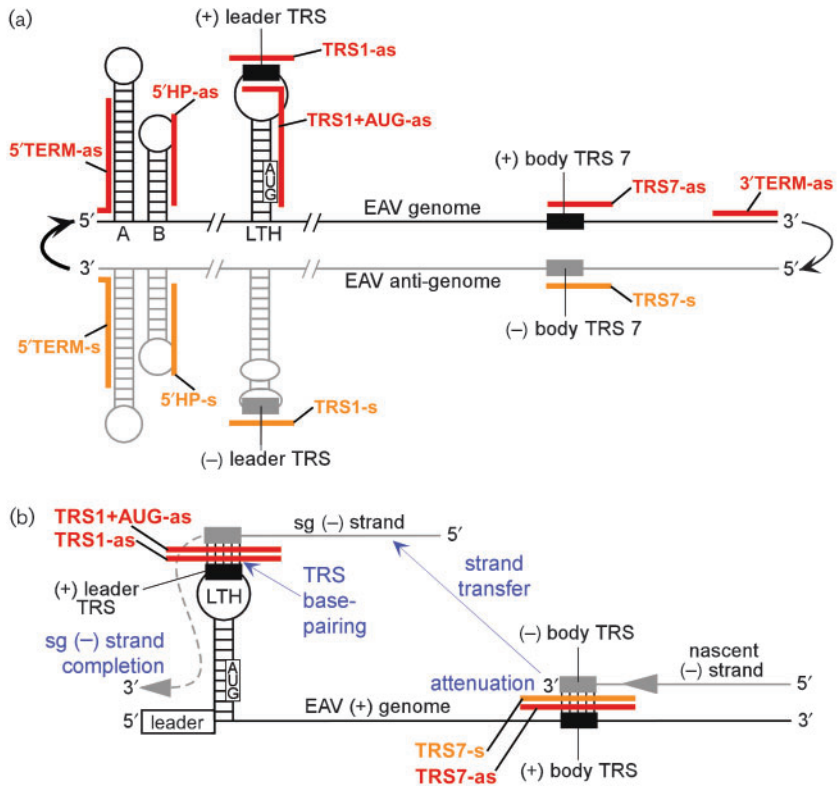


**Fig. 1.** Overview of EAV P-PMO target locations. (a) Schematic overview of the position of the P-PMO targets in the EAV genome and antigenome (antisense and sense P-PMOs are depicted in red and orange, respectively). Elements from the previously described structure model for the 5′-proximal region of the genome are depicted (van den Born *et al.*, 2004). The RNA structures drawn in the minus-strand (grey) are hypothetical and have not been demonstrated via structure probing. Depicted are the 5′-terminal hairpin A, the conserved hairpin B and the leader TRS hairpin (LTH). The black boxes indicate the position of the leader TRS and RNA7 body TRS in the genome; the grey boxes indicate the corresponding complementary sequences in the antigenome. (b) P-PMOs designed to interfere with discontinuous minus-strand synthesis (see text for details). P-PMOs TRS1-as, TRS7-s and TRS1+AUG-as were designed to interfere with the leader TRS-to-body TRS base-pairing step.

sequences in the positive-strand genomic 5′ UTR efficiently reduced virus amplification in a dose-responsive manner. At concentrations in the low micromolar range, some of these compounds completely, and others near-completely, inhibited virus amplification. *In vitro* translation assays indicated that these P-PMOs likely inhibited genome translation. Our data suggest that several of these compounds have antiviral potential at relatively low concentrations and also represent useful tools to study the molecular biology of arteriviruses.

## METHODS

**Cells and viruses.** Vero-E6 cells were cultured in Dulbecco's modified Eagle's medium (DMEM) containing 8 % fetal calf serum (FCS) for maintenance, or in DMEM without FCS or with 4 % FCS, as stated, during P-PMO studies. EAV–GFP (green fluorescent protein) (see below for details) and *Sindbis virus* (SinV; HR strain) were both propagated in Vero-E6 cells at 37 °C. Virus titration using plaque assays was as described previously (Molenkamp *et al.*, 2000a).

**RNA isolation and analysis.** Intracellular RNA from Vero-E6 cells was isolated at 36 h post-infection (p.i.), separated in denaturing agarose formaldehyde gels and analysed by hybridization to a $^{32}$P-labelled probe, which is complementary to the 3′ end of the EAV genome and all sg mRNAs (5′-TTGGTTCCTGGGTGGCTAATAACTACTT-3′) (van Marle *et al.*, 1999). Dried gels were exposed to phosphorimager screens and scanned with a Personal Molecular Imager FX (Bio-Rad) after exposure. Band intensities were quantified with Quantity One v4.2.2 (Bio-Rad).

**P-PMO design and synthesis.** Morpholino oligomers were designed to be complementary to target sequences in the EAV genome or antigenome. See Table 1, Fig. 1 and Results for P-PMO sequences and target locations. PMO is a single-stranded DNA analogue that has a morpholine ring in place of each riboside moiety and phosphorodiamidate intersubunit linkages instead of phosphorodiester linkage (Summerton & Weller, 1997). The nucleoside bases attached to this backbone are the same as for DNA. In order to deliver the PMOs into cultured cells, an arginine-rich peptide $NH_2$-RRRRRRRRRFF-$CONH_2$, designated $R_9F_2C$ (Moulton *et al.*, 2004), was covalently linked to the 5′ end of each PMO. The performance of the $R_9F_2C$ peptide varies with the amount of serum in the media (Neuman *et al.*, 2004; Moulton *et al.*, 2004). Hence, the 6 h P-PMO treatments were carried out in the absence of serum. All PMOs were synthesized at AVI BioPharma by methods described previously (Summerton & Weller, 1997). The conjugation, purification and analysis of P-PMO compounds were carried out at AVI BioPharma according to methods described elsewhere (Moulton *et al.*, 2004).

**P-PMO studies.** Vero-E6 cells were grown to approximately 80 % confluence. For pre-treatment experiments, Vero-E6 cells were incubated for 6 h in serum-free DMEM containing different concentrations of P-PMOs. After removal of the medium and washing, the cells were infected with EAV–GFP or SinV at an m.o.i. of 0·5 p.f.u. per cell for 1 h. Subsequently, the inoculum was removed and fresh DMEM containing 4 % FCS was added. For post-treatment experiments, Vero-E6 cells were infected as above, the inoculum was then removed, the cells rinsed and P-PMO treatment applied for 6 h, after which the compound was not removed but 1 vol. fresh medium was added, resulting in a final concentration of FCS of 4 %. As a consequence, the residual concentration of P-PMOs was halved.

**Translation assays.** To test the effect of various P-PMOs on translation, cell-free translation assays were carried out using the previously described pDualLuc-scan1 reporter gene construct for EAV genome translation (van den Born *et al.*, 2005). *In vitro* transcribed, capped bicistronic DualLuc-scan1 transcripts were *in vitro* translated in the presence of various P-PMOs using the Rabbit Reticulocyte Lysate system according to the manufacturer's protocol (Promega). Luciferase expression was measured using a luminometer (Turner Designs TD-20/20) and the Dual-Luciferase Reporter assay (Promega) on the basis of enzymic activity.

## RESULTS

### Design of P-PMOs targeting EAV RNA sequences involved in replication, sg mRNA synthesis and translation

It has been established that the efficient replication of many RNA viruses requires essential sequence and structural elements in terminal regions of the genome and antigenome, which are recognized by the viral RNA-dependent RNA

**Table 1.** P-PMO details

| P-PMO | Target in EAV | P-PMO polarity | P-PMO sequence (5′–3′) | Position* | $IC_{50(GFP)}$ (μM)† |
|---|---|---|---|---|---|
| 5′TERM-as | Genomic 5′ terminus | Antisense | GCACCATACACACTTCGAGC | 1–20 | 1·5 |
| 5′TERM-s | Antigenomic 3′ terminus | Sense | GCTCGAAGTGTGTATGGTGC | 1–20 | 6·5 |
| 5′HP-as | Conserved hairpin in 5′ UTR | Antisense | GGCCCACAAGAATAGTAATT | 53–72 | 3 |
| 5′HP-s | Conserved hairpin in 5′ UTR complement | Sense | AATTACTATTCTTGTGGGCC | 53–72 | 10 |
| TRS1-as | (+) leader TRS | Antisense | AAGGGTAGTTGATAGAGATC | 199–218 | 3 |
| TRS1-s | (−) leader TRS | Sense | GATCTCTATCAACTACCCTT | 199–218 | >20 |
| TRS1+AUG-as | (+) leader TRS and replicase initiator AUG | Antisense | CCATAGTCGCAAGGGTAGTTGA | 207–228 | 2 |
| TRS7-as | (+) RNA7 body TRS | Antisense | ACCACTACCTGAGTAGTTGA | 12252–12271 | 7 |
| TRS7-s | (−) RNA7 body TRS | Sense | TCAACTACTCAGGTAGTGGT | 12252–12271 | 20 |
| 3′TERM-as | Genomic 3′ terminus | Antisense | GGTTCCTGGGTGGCTAATAACT | 12683–12704 | 10 |
| SCR | Nonsense (control) | – | AGTCTCGACTTGCTACCTCA | – | >20 |

*Location of the target sequence in the EAV genome (GenBank accession no. NC_002532).

†Approximate P-PMO concentration generating 50 % reduction in the number of eGFP-positive cells; derived from Fig. 3(b).

polymerase (RdRp) complex (Panavas *et al.*, 2002; Tortorici *et al.*, 2003). Specifically, the RdRp complex interacts with the 3′ end of the genome and antigenome to initiate the synthesis of minus- and plus-strands, respectively (Fig. 1a). In an attempt to interfere with such interactions, P-PMOs complementary to the 3′ end of the genome (3′TERM-as) and antigenome (5′TERM-s) were designed. A previous analysis of the secondary structure of the 5′-proximal 300 nt of the EAV genome revealed that the 5′ UTR contains an RNA hairpin that is conserved among different EAV isolates and is predicted to occur in both the plus and the minus-strand conformations (hairpin B; Fig. 1a) (van den Born *et al.*, 2004). Because of its sequence and structural conservation and its close proximity to the 3′ end of the antigenome, it likely plays a role in the initiation of plus-strand synthesis. Two P-PMOs were designed to disrupt this RNA structure either in the plus- or in the minus-strand (5′HP-as and 5′HP-s, respectively).

To assess whether using P-PMOs could reduce the synthesis of sg mRNAs, several TRS motifs were targeted (Fig. 1b). PMO–TRS interactions were expected to interfere with body TRS-to-leader TRS base pairing, which is a crucial step in the production of sg RNAs (van Marle *et al.*, 1999; Pasternak *et al.*, 2001). The leader TRS of EAV is predicted to be located in the 20 nt loop of the so-called leader TRS hairpin (LTH; Fig. 1). One P-PMO was complementary to the entire LTH loop (TRS1-as), whereas another P-PMO spanned both the leader TRS and the downstream replicase translation initiation codon (TRS1 + AUG-as). A P-PMO complementary to TRS1-as (TRS1-s) was an appropriate control in these transcription-inhibition studies, as it was designed to target the complement of the leader TRS which is not involved in TRS base pairing. In addition, the RNA7 body TRS was targeted with two P-PMOs designed to interfere specifically with sg RNA7 synthesis. One P-PMO (TRS7-as) was complementary to the RNA7 body TRS in the genomic template and was designed to interfere with the attenuation step that has been postulated to precede the discontinuous step during sg minus-strand RNA synthesis. The other (TRS7-s) was designed to anneal to the RNA7 body TRS complement at the 3′ end of the nascent minus-strand that, following attenuation, is presumed to be translocated to and base pair with the leader TRS.

Four of the P-PMOs were designed against targets located in the genomic 5′ UTR. In addition to the 5′HP-as, TRS1-as and TRS1 + AUG-as compounds, described above, a P-PMO with a sequence antisense to the 5′-terminal 20 nt (5′TERM-as) was designed to interfere with pre-initiation of translation of all sg mRNAs and genomic mRNA. Although P-PMO TRS1 + AUG-as (Fig. 1a) was designed to interfere with genome translation (as well as sg mRNA synthesis) it is the only one of the four with little likelihood of interfering with sg mRNA translation, as all sg mRNAs lack most of the 16 contiguous nucleotides immediately downstream of the leader TRS that are part of the TRS1 + AUG-as target sequence (den Boon *et al.*, 1996). In contrast, translation of all sg mRNAs and genomic RNA could be affected by 5′TERM-as and 5′HP-as as they target sequences in the common leader. A ‘nonsense’ P-PMO (SCR) was also synthesized as a control for off-target effects of the P-PMO chemistry. P-PMO design details are summarized in Table 1.

## P-PMOs display low cytotoxicity and have EAV-specific antiviral activity

A cytotoxicity assay was performed in which each P-PMO was tested on Vero-E6 cells at concentrations of 0, 5, 10, 20, 40 or 80 μM in the culture medium. Cells were cultured with P-PMOs for 6 h in the absence of serum to allow P-PMO uptake, after which P-PMO-free medium containing 8 % FCS was given. Cell proliferation was monitored by microscopy after 3 days of incubation. At the highest concentration (80 μM) some of the P-PMOs clearly affected cell growth, as was evident from the reduced cell density compared with untreated cells. At 40 μM no morphological growth anomalies were apparent (data not shown), but as a precaution the P-PMO concentration never exceeded 20 μM in any subsequent experiment.

To assess P-PMO specificity and cytotoxicity, the effect of each compound on EAV amplification was compared to its effect on the amplification of the (unrelated) togavirus SinV. Cells were post-treated with 20 μM of each P-PMO, following inoculation with EAV or SinV under identical cell culture conditions, and virus yields were measured at 36 or 24 h p.i., respectively. SinV titres in the untreated control reached approximately $10^6$ p.f.u. $ml^{-1}$ and were not significantly altered by P-PMO treatment (Fig. 2). Remarkably, several P-PMOs reduced the EAV titre by several orders of magnitude or even to undetectable levels (Fig. 2). At 20 μM, control P-PMO SCR induced an approximately threefold reduction in EAV titre, an effect that was not observed with SinV. However, the much stronger anti-EAV effect observed with most EAV-targeted P-PMOs was clearly specific and

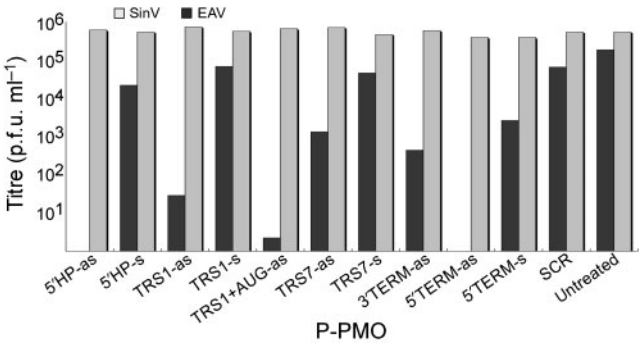


**Fig. 2.** Evaluation of the efficacy and specificity of EAV-targeted P-PMOs. Cells were infected with EAV or SinV, then treated with P-PMO at a final concentration of 20 μM in the media. Virus titres (p.f.u. $ml^{-1}$) were determined by plaque assays.

not due to cytotoxicity or a generic barrier to cellular entry or egress of virus, as such non-specific effects would likely have caused an inhibition of SinV amplification as well.

## Rapid evaluation of P-PMO efficacy using a GFP-expressing recombinant EAV

To facilitate the screening for P-PMO inhibitory effects, a novel recombinant EAV (EAV–GFP) was used. A detailed description of EAV–GFP will be published elsewhere (E. van den Born, H. van den Berg and E. J. Snijder, unpublished data). Briefly, EAV–GFP expresses enhanced green fluorescent protein (eGFP) as an integral part of the replicase polyproteins through an in-frame insertion at the position in ORF1a specifying the nsp1/nsp2 cleavage site of a cassette (eGFP/2A) consisting of the eGFP-coding sequence and the *Foot-and-mouth disease virus* 2A autoprotease. The nsp1-eGFP/2A junction is cleaved by the nsp1 autoprotease, whereas the 2A sequence can release the N terminus of nsp2. Replication of EAV–GFP was not significantly affected by the eGFP insertion, and its growth characteristics and virus titres were comparable to that of wild-type EAV (data not shown). EAV–GFP-infected cells were readily detected by microscopy through eGFP autofluorescence (Fig. 3a), which allowed us to quickly screen a wide concentration range of P-PMO. Most of the eGFP expressed by EAV–GFP co-localized with other non-structural proteins in the perinuclear region of the cell (data not shown), whereas a small proportion was distributed throughout the cytoplasm (Fig. 3a). A number of comparative studies using wild-type EAV and EAV–GFP showed that the titre of both viruses was similarly affected by a given P-PMO concentration (data not shown), thus validating the use of EAV–GFP for the inhibition assays in this study. Consequently, the recombinant virus was used throughout the experiments described in this report.

To further assess the efficacy of the various P-PMOs, cells were given medium with a final concentration of 0, 1, 2, 4, 10 or 20 μM of one of the compounds for 6 h prior to (pre-treatment) or following (post-treatment) EAV–GFP infection at an m.o.i. of 0·5. Intracellular eGFP expression was visually monitored at 36 h p.i. by microscopy, which revealed that several P-PMOs affected the percentage of virus-infected cells, but that individual cells that were eGFP-positive did not exhibit much variation in eGFP expression level (Fig. 3a). Intermediate eGFP expression was observed only in one case, when cells were treated with 3′TERM-as, although it should be noted that visual observation via microscopy is not truly a quantitative method. P-PMO pre-treatment resulted in an approximate twofold stronger inhibition than post-treatment. However, only post-treatment was used in subsequent

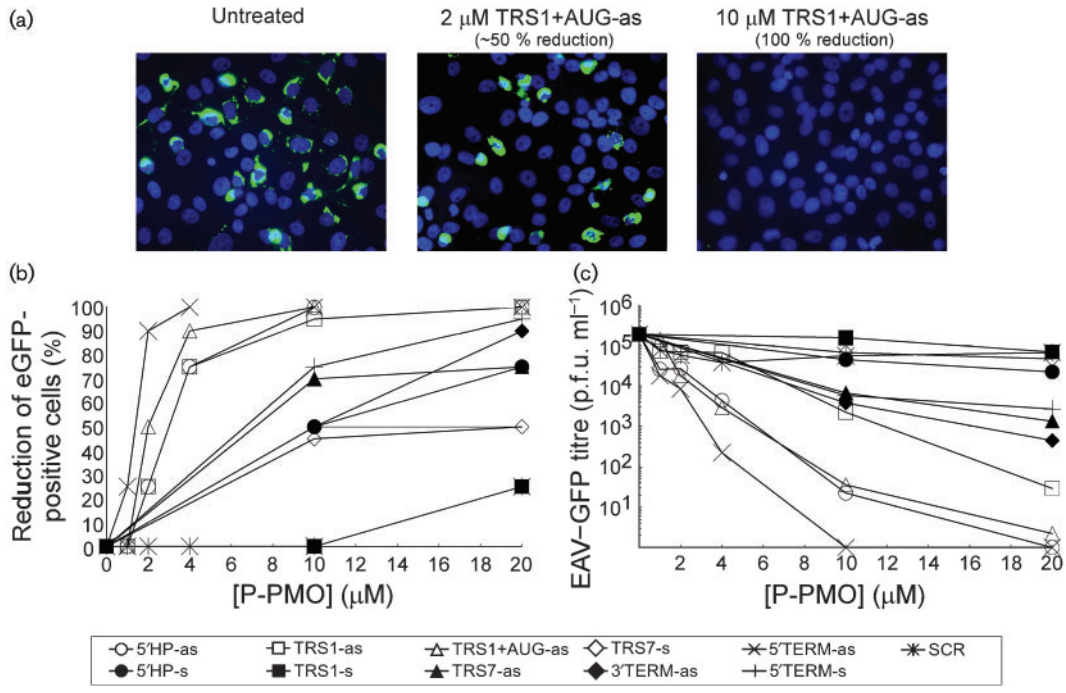


**Fig. 3.** Dose-response evaluation of the antiviral activity of P-PMOs. (a) Example of reduction in the number of EAV–GFP-positive cells due to P-PMO (TRS1 + AUG-as) treatment as monitored by GFP-autofluorescence microscopy. Nuclei were labelled by Hoechst staining. (b) The reduction in the number of eGFP-positive cells observed microscopically, which is indicative of the inhibition of EAV–GFP amplification, plotted against the P-PMO treatment concentration used. (c) Cell culture medium from the experiment in (b) was harvested at 36 h p.i. and virus titres (p.f.u. $ml^{-1}$) were determined by plaque assay.

experiments, for reasons explained in the Discussion. Remarkably, a 25-fold m.o.i. increase (to m.o.i. 12·5) did not affect the number of eGFP-positive cells present after a P-PMO treatment of any given concentration (data not shown). This finding indicated that the protective effect of a P-PMO was not overcome when cells were challenged with higher virus concentrations.

The P-PMOs could be divided into three groups based on their ability to reduce the number of eGFP-positive cells. The first group consisted of TRS1-s and SCR, both of which had almost no effect on EAV–GFP amplification when compared to the untreated control cells. At the highest P-PMO concentration used (20 μM), a relatively small reduction of about 25 % in the number of eGFP-positive cells was observed (Fig. 3b). A second P-PMO group, exhibiting intermediate efficacy, consisted of 5′HP-s, TRS7-as, TRS7-s, 3′TERM-as and 5′TERM-s, which, at relatively high compound concentrations, protected the majority (50–95 %) of cells (Fig. 3b). The third group comprises the four most active P-PMOs. Three of these compounds (5′HP-as, TRS1 + AUG-as and 5′TERM-as) when present at 10 μM, and the fourth (TRS1-as) at 20 μM, were able to apparently protect all cells from virus infection (Fig. 3b). In summary, most of the P-PMOs generated a substantial degree of inhibition of virus amplification when administered to cells immediately after virus infection.

## Several P-PMOs inhibit virus amplification in a dose-dependent manner

To quantify the relationship between dose and efficacy of the various P-PMOs, cells were post-treated at varying P-PMO concentrations for 6 h following EAV–GFP infection. Virus titres in cell culture media harvested at 36 h p.i. were determined by plaque assays. Not unexpectedly, the relative titre reductions observed with the different P-PMO dose levels (Fig. 3c) were in agreement with the relative number of infected cells determined by eGFP autofluorescence (Fig. 3b). The group of four P-PMOs with the highest inhibition efficiency (5′HP-as, TRS1 + AUG-as, 5′TERM-as, and to a lesser extent TRS1-as) generated EAV–GFP titre reductions of four logs or greater, from a peak titre of $2{\cdot}0 \times 10^5$ p.f.u. $ml^{-1}$ in untreated cells, to 30 p.f.u. $ml^{-1}$ or below in treated cells. These four compounds are all complementary to sequences in the genomic 5′ UTR, indicating that this region is the most effectual target area for this class of compounds, at least in EAV. It is noteworthy that the small amount of residual virus from the inoculum that is usually detectable in low dilutions of culture medium, was not recovered in plaque assays (Fig. 3c; see also Fig. 2). The most likely explanation is that even residual amounts of highly efficacious P-PMOs prevented detectable plaque formation. Therefore, the P-PMO concentration at which virus particle production was completely prevented could not be exactly determined.

Some of the P-PMOs that do not have target sequences in the 5′ UTR were able to inhibit virus amplification in a dose-dependent manner, but significant effects were observed only at relatively high concentrations ($\geqslant$10 μM). TRS1-s, which targets the leader TRS complement, was completely ineffective (Fig. 3b and c). Moderate effects of up to one log-reduction were observed for 5′HP-s and TRS7-s (Fig. 3c), both of which target the minus-strand. The result obtained with 5′HP-s was particularly interesting because it targeted the complement of the conserved hairpin B in the 5′ UTR (Fig. 1a), suggesting that this sequence (and/or putative structure), located in the 3′ end of the antigenome, plays a role in genome replication. Fairly strong inhibitory effects of approximately two log-reduction were obtained with 3′TERM-as, 5′TERM-s and TRS7-as. The former two target the 3′ terminus of the genome and antigenome, respectively, and these results suggest that they interfere with the interaction between EAV RNA and the replicase complex.

## P-PMOs targeting the EAV 5′ UTR can markedly interfere with translation

To investigate the effect of the above-identified highly active compounds on EAV genome translation, a cell-free translation assay was performed using the previously described pDualLuc-scan1 construct (van den Born *et al.*, 2005). Briefly, the T7 promoter of this vector directs the synthesis of a bicistronic mRNA harbouring the EAV 5′ UTR fused to the firefly luciferase ($F_{luc}$) reporter gene followed by an *Encephalomyocarditis virus* (EMCV) IRES-driven *Renilla* luciferase ($R_{luc}$) gene, which serves as an internal standard in the experiments. *In vitro* transcribed, capped DualLuc-scan1 mRNA was added to rabbit reticulocyte lysate and the translation of the two reporter genes was measured. The expression of both $F_{luc}$ and $R_{luc}$ was analysed in the presence of the P-PMOs targeting the 5′ UTR (5′TERM-as, 5′HP-as, TRS1 + AUG-as and TRS1-as), SCR and 3′TERM-as. The latter compound is complementary to the 3′-terminal region of the EAV genome that is also present in DualLuc-scan1 mRNA (Fig. 4a). Unless mRNA circularization is required for efficient translation *in vitro*, 3′TERM-as would not be expected to have activity in this system. At the highest P-PMO concentration used in this assay (1 μM), expression from the $R_{luc}$ control cistron was not affected and could be used to normalize the $F_{luc}$ activity (Fig. 4b). At nanomolar concentrations all P-PMOs targeting the 5′ UTR generated dose-dependent reduction of $F_{luc}$ expression, with a 50 % inhibition concentration ($IC_{50}$) in the 10–100 nM range. Both controls, the SCR and 3′TERM-as P-PMOs, did not show nearly as high a reduction in translation, with $IC_{50}$ values of approximately 1000 nM (Fig. 4c).

## P-PMOs are unable to specifically affect sg mRNA synthesis

The discontinuous minus-strand extension model for sg RNA synthesis (Sawicki & Sawicki, 1995) defined several interesting targets for antisense studies. P-PMOs TRS1-as, TRS1 + AUG-as, TRS1-s, TRS7-s and TRS7-as were

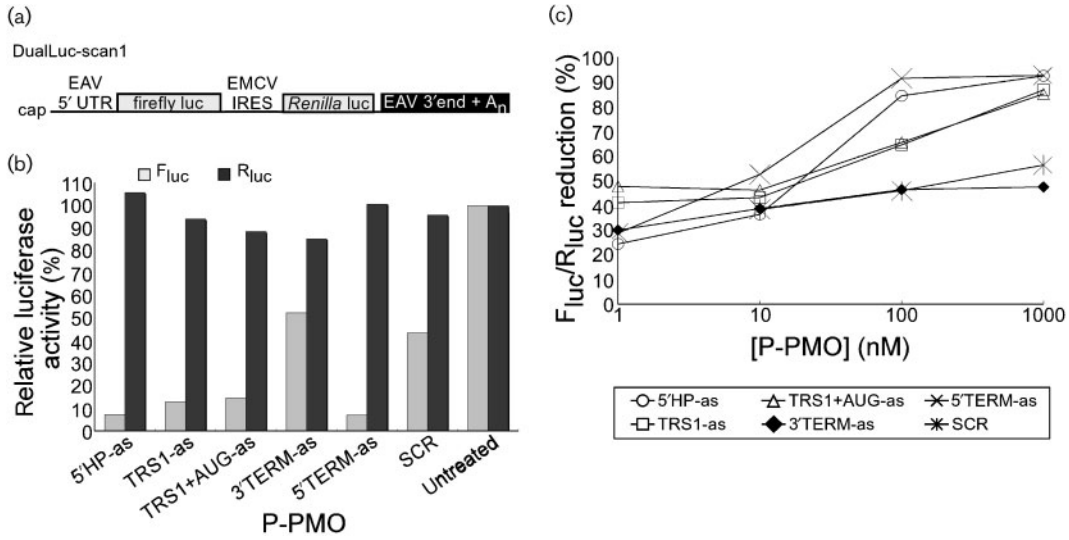


**Fig. 4.** Analysis of translation inhibition by P-PMOs targeting the 5′ UTR of the EAV genome. (a) Schematic representation of the DualLuc-scan1 mRNA reporter (van den Born *et al.*, 2005). Depicted are the EAV genomic 5′ UTR, the $F_{luc}$ reporter gene, the EMCV IRES element that drives $R_{luc}$ expression, the $R_{luc}$ gene (internal standard) and the 3′-terminal region of the EAV genome [starting from nt 11737 and including a poly(A) tail]. (b) Cell-free translation assay using DualLuc-scan1 mRNA in the presence of 1 μM P-PMOs. The $F_{luc}$ and $R_{luc}$ expression relative to that of the untreated control are presented. (c) Cell-free translation assay. The $F_{luc}$ activity was normalized to the $R_{luc}$ activity and the decrease in this ratio relative to that of the untreated control was plotted against the P-PMO concentration.

designed to affect sg RNA synthesis by interfering with leader TRS-to-body TRS base pairing. Notably, the first two of these P-PMOs inhibited virus amplification likely by interfering with translation, whereas TRS7-as probably affected genome replication. To assess the effect of these P-PMOs on sg RNA production, EAV–GFP-infected cells were treated with P-PMO at the concentration that gives 50 % reduction of GFP-positive cells ($IC_{50(GFP)}$; Table 1), which should reveal any major effects on viral sg mRNA synthesis. Intracellular RNA was isolated at 36 h p.i. and subjected to hybridization analysis (Fig. 5a). The band intensities for genomic RNA and the three major sg mRNAs (2, 6 and 7) were measured by phosphorimager analysis. For each lane the ratio of sg RNA to genome synthesis was calculated and depicted in Fig. 5(b). Although, due to common variation in experimental procedures, some fluctuation in this ratio was observed, none of the TRS-specific P-PMOs showed a specific reduction in the synthesis of all sg mRNAs (TRS1-as and TRS1 + AUG-as) or sg mRNA7 (TRS7-as and TRS7-s).

## DISCUSSION

Employing morpholino oligomers to inhibit RNA virus amplification has become an appealing prospect after many reports of the successful knockdown of cellular proteins via inhibition of pre-mRNA splicing and/or translation of mRNAs (Nasevicius & Ekker, 2000; Liu *et al.*, 2003; Boguslavsky *et al.*, 2003; Muto *et al.*, 2004). RNA virus genomes offer a variety of interesting regions for PMO-targeting other than the 5′ UTR, which is ordinarily selected for the purpose of inhibiting translation. Recently, two studies reported that P-PMOs targeted to RNA *cis*-acting elements involved in flavivirus genome replication successfully suppressed virus amplification (Kinney *et al.*, 2005; Deas *et al.*, 2005). In our study, we tested the ability of several P-PMOs to inhibit virus amplification by targeting RNA elements involved in three different aspects of the EAV life cycle: replication, sg mRNA synthesis and translation. Importantly, the P-PMOs generated little cytopathic effects at concentrations lower than 40 μM, as assessed by cell proliferation assays. Moreover, SinV growth was not suppressed by any of the P-PMOs and the post-infection treatment protocol used in all of our experiments (Fig. 2).

The 5′ UTR of the EAV genome was found to contain the most sensitive targets for inhibition with P-PMOs (Table 1 and Fig. 1). All four P-PMOs directed to the 5′ UTR were able to profoundly inhibit EAV amplification at low micromolar concentrations (Fig. 3b and c), with the P-PMO targeting the 5′ genomic terminus (5′TERM-as) consistently generating the strongest effect. For arteriviruses and coronaviruses, the genomic 5′ UTR provides an appealing target area, because all viral mRNA share a large part of this region, the common leader sequence, due to the unique mechanism of sg RNA synthesis. Consequently, P-PMOs 5′TERM-as and 5′HP-as may inhibit the translation of replicase-coding EAV genomic RNA as well as all six sg mRNAs. *In vitro* translation assays indicated that their

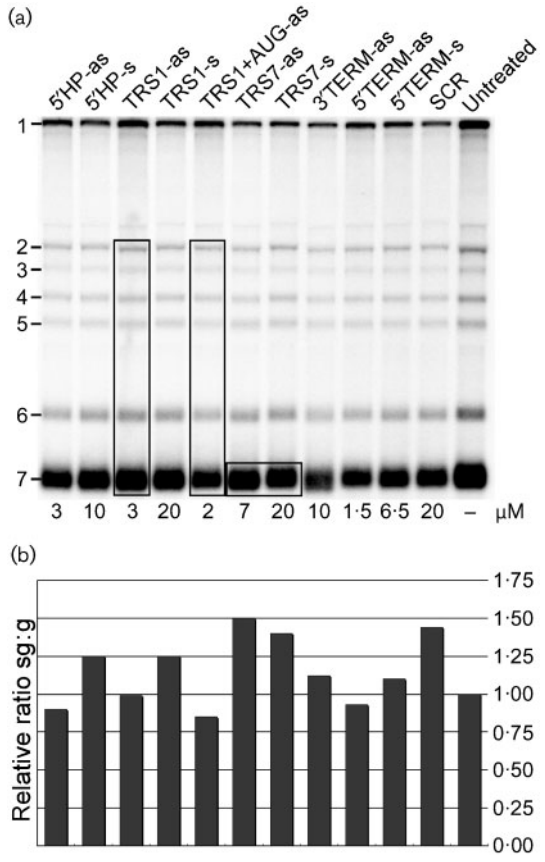


**Fig. 5.** Effect of P-PMO treatment on EAV RNA synthesis. (a) Gel hybridization analysis of EAV-specific mRNAs isolated at 36 h p.i. from EAV–GFP-infected Vero-E6 cells. P-PMOs were added at the $IC_{50(GFP)}$ level previously determined for each of them (Table 1). The P-PMO concentration used is indicated below each lane. The position of the RNAs is indicated: 1, genome RNA; 2–7, sg mRNAs. Four P-PMOs were targeted to TRSs (leader TRS or RNA7 body TRS) in an attempt to specifically reduce synthesis of the sg mRNAs that are boxed. (b) Quantification of viral RNA synthesis upon P-PMO treatment, based on the hybridization experiment shown in panel (a). The amount of sg mRNAs was normalized to that of the genome. This ratio (sg : g) was compared with that of the untreated control, which was set to 1.

antiviral effect was exerted, at least partly, by inhibition of translation (Fig. 4). A cell culture-based translation assay was also attempted, using transient expression of the luciferase reporters driven by the cytomegalovirus promoter that is present, in addition to the T7 promoter, in pDualLucscan1. However, for unexplained reasons, P-PMO treatment equally affected the expression of both $F_{luc}$ and the internal standard $R_{luc}$ in a sequence-specific and dose-dependent manner (data not shown). This suggested a problem with plasmid DNA transfection or reporter mRNA synthesis or stability in the presence of P-PMO and, consequently, we had to refrain from using this assay.

Our results indicate that genome replication can also be reduced by targeting the genome termini (P-PMOs: 3′TERM-as and 5′TERM-s). Since translation assays indicated that the mode of action of 3′TERM-as was unlikely to be through interference with translation (Fig. 4), we assumed that it exerted its inhibitory effect by acting on particular events during RNA synthesis. Rather unexpectedly, TRS7-as also significantly suppressed virus amplification (Fig. 3c), despite its target sequence being located approximately 450 nt from the genomic 3′ end. Whether the P-PMO duplexing to this target affected the initiation of replication or perhaps blocked the processing RdRp complex is unclear.

No effect on sg mRNA synthesis was observed when leader or body TRS motifs were targeted. A likely explanation is that the target sequences for these P-PMOs were not accessible due to RNA structural or intracellular ultrastructural constraints. Genome replication and sg mRNA synthesis are thought to occur in association with dedicated double membrane vesicles that are believed to provide a suitable platform for viral RNA synthesis (Pedersen *et al.*, 1999). This protective microenvironment may physically prevent P-PMOs from entering replication complexes. Incoming viral genomes, which are translated in the cytoplasm in a similar manner to cellular mRNAs, are likely to be more accessible and thus susceptible to antisense P-PMO hybridization. Another possibility is that virus-encoded enzymes such as the nsp10 helicase can displace the P-PMO during sg RNA synthesis prior to the interaction between the leader TRS and the body TRS.

In all our experiments a post-treatment procedure was performed, although it has been found to be less effective compared with pre-treatment (Kinney *et al.*, 2005). However, we encountered several undesired side effects when using a P-PMO pre-treatment, probably due to the positively charged arginine-rich peptide conjugate. Firstly, to a certain extent, pre-treatment with P-PMOs protected cells against virus infection, an observation that was made for both EAV and SinV. This non-specific effect was also noted in a previous study (Kinney *et al.*, 2005). Secondly, in some cases high P-PMO concentrations actually increased virus titres as determined by plaque assays. For example, at both 4 and 10 μM of 5′TERM-as there were no eGFP-positive cells detected, but the amount of residual virus from the inoculum recovered from the 10 μM sample was approximately ten times higher than in the 4 μM sample (data not shown). This suggested that virus particles from the inoculum may adhere to the outside of cells pre-treated with certain P-PMO concentrations more than they do to non-treated cells. Finally, in cell culture-based translation studies, the efficiency of cationic-lipid mediated plasmid DNA transfection appeared to be influenced by P-PMO (data not shown). P-PMOs have been shown to accumulate in cellular membranes (Moulton *et al.*, 2003, 2004). This accumulation of charged molecules may interfere with virus entry (and release) as well as cationic-lipid uptake. A

post-infection P-PMO treatment strategy can be recommended to avoid these problems, and was done for all the experiments reported here.

We consistently observed that for any individual cell P-PMO treatment using our eGFP-expressing EAV–GFP recombinant generally resulted in an 'all or nothing' outcome of infection. Either eGFP expression was completely absent, indicating that EAV–GFP was not able to replicate, or a bright fluorescence was observed, indicating that a vigorous virus infection was in progress. This phenomenon could be explained by low-level EAV–GFP replication in the presence of P-PMO, slowly generating more and more viral RNA. At some point, the number of viral targets could reach a threshold level over which the number of P-PMO molecules becomes inconsequential, allowing the virus to replicate robustly.

P-PMOs appear to have some potential as antisense therapeutics *in vivo*. They behave with predictability and potency, and displayed little non-specificity in most of our systems. The ability of a post-infection P-PMO treatment to significantly reduce the degree of viral amplification further supports the idea that this class of compounds may be suitable for therapeutic development. Delivery of PMOs into cells can clearly be enhanced by using peptide conjugation, which may prove to be an important factor in future drug design. One obstacle may be that serum reduces the cellular uptake of the type of arginine-rich peptide used in this study (Neuman *et al.*, 2004). However, new types of peptide conjugates may be able to overcome this problem (Deas *et al.*, 2005).

Arteriviruses and coronaviruses are a major economic problem in the swine and cattle breeding industry, and coronaviruses also cause a considerable amount of human disease, such as severe acute respiratory syndrome and a substantial percentage of cases of the common cold syndrome (Saif *et al.*, 1988; Albina, 1997; Makela *et al.*, 1998; Cook, 2002; Peiris *et al.*, 2003). The arterivirus EAV has proven to be a safe and convenient tool to study various aspects of nidovirus molecular biology, in particular viral RNA synthesis and replicase function. Continued *in vitro* studies and *in vivo* approaches with various types of P-PMOs will be required to assess the potential of these compounds to protect against and/or treat diseases caused by nidoviruses. In any case, it is clear from this study that these compounds represent useful reagents for exploring various aspects of molecular virology, especially translation mechanics.

## ACKNOWLEDGEMENTS

We would like to thank the Chemistry Department at AVI BioPharma for expert synthesis, purification and analysis of peptide-PMOs. We appreciate the technical assistance of Karin Wever and Erik van den Berg in the construction of the EAV–GFP recombinant. E. B. was supported by Council for Chemical Sciences grant CW 99-010 from The Netherlands Organization for Scientific Research.

## REFERENCES

**Albina, E. (1997).** Epidemiology of porcine reproductive and respiratory syndrome (PRRS): an overview. *Vet Microbiol* **55**, 309–316.

**Boguslavsky, D., Ierusalimsky, V., Malyshev, A., Balaban, P. & Belyavsky, A. (2003).** Selective blockade of gene expression in a single identified snail neuron. *Neuroscience* **119**, 15–18.

**Cook, J. (2002).** In *Poultry Diseases*, 5th edn, pp. 298–306. Edited by F. Jordan, M. Pattison, D. Alezander & T. Faragher. London: W. B. Saunders.

**Deas, T. S., Binduga-Gajewska, I., Tilgner, M. & 7 other authors (2005).** Inhibition of flavivirus infections by antisense oligomers specifically suppressing viral translation and RNA replication. *J Virol* **79**, 4599–4609.

**den Boon, J. A., Kleijnen, M. F., Spaan, W. J. M. & Snijder, E. J. (1996).** Equine arteritis virus subgenomic mRNA synthesis: analysis of leader-body junctions and replicative-form RNAs. *J Virol* **70**, 4291–4298.

**González, J. M., Gomez-Puertas, P., Cavanagh, D., Gorbalenya, A. E. & Enjuanes, L. (2003).** A comparative sequence analysis to revise the current taxonomy of the family *Coronaviridae*. *Arch Virol* **148**, 2207–2235.

**Heasman, J. (2002).** Morpholino oligos: making sense of antisense? *Dev Biol* **243**, 209–214.

**Jubin, R., Vantuno, N. E., Kieft, J. S., Murray, M. G., Doudna, J. A., Lau, J. Y. & Baroudy, B. M. (2000).** Hepatitis C virus internal ribosome entry site (IRES) stem loop IIId contains a phylogenetically conserved GGG triplet essential for translation and IRES folding. *J Virol* **74**, 10430–10437.

**Kinney, R. M., Huang, C. Y., Rose, B. C., Kroeker, A. D., Dreher, T. W., Iversen, P. L. & Stein, D. A. (2005).** Inhibition of dengue virus serotypes 1 to 4 in vero cell cultures with morpholino oligomers. *J Virol* **79**, 5116–5128.

**Liu, Y., Sinha, S. & Owens, G. (2003).** A transforming growth factor-$\beta$control element required for SM $\alpha$-actin expression *in vivo* also partially mediates GKLF-dependent transcriptional repression. *J Biol Chem* **278**, 48004–48011.

**Makela, M. J., Puhakka, T., Ruuskanen, O., Leinonen, M., Saikku, P., Kimpimaki, M., Blomqvist, S., Hyypia, T. & Arstila, P. (1998).** Viruses and bacteria in the etiology of the common cold. *J Clin Microbiol* **36**, 539–542.

**McCaffrey, A. P., Meuse, L., Karimi, M., Contag, C. H. & Kay, M. A. (2003).** A potent and specific morpholino antisense inhibitor of hepatitis C translation in mice. *Hepatology* **38**, 503–508.

**Molenkamp, R., Greve, S., Spaan, W. J. M. & Snijder, E. J. (2000a).** Efficient homologous RNA recombination and requirement for an open reading frame during replication of equine arteritis virus defective interfering RNAs. *J Virol* **74**, 9062–9070.

**Molenkamp, R., Rozier, B. C., Greve, S., Spaan, W. J. M. & Snijder, E. J. (2000b).** Isolation and characterization of an arterivirus defective interfering RNA genome. *J Virol* **74**, 3156–3165.

**Molenkamp, R., van Tol, H., Rozier, B. C., van der Meer, Y., Spaan, W. J. M. & Snijder, E. J. (2000c).** The arterivirus replicase is the only viral protein required for genome replication and subgenomic mRNA transcription. *J Gen Virol* **81**, 2491–2496.

**Moulton, H. M., Hase, M. C., Smith, K. M. & Iversen, P. L. (2003).** HIV Tat peptide enhances cellular delivery of antisense morpholino oligomers. *Antisense Nucleic Acid Drug Dev* **13**, 31–43.

**Moulton, H. M., Nelson, M. H., Hatlevig, S. A., Reddy, M. T. & Iversen, P. L. (2004).** Cellular uptake of antisense morpholino oligomers conjugated to arginine-rich peptides. *Bioconjug Chem* **15**, 290–299.

**Muto, E., Tabata, Y., Taneda, T., Aoki, Y., Muto, A., Arai, K. & Watanabe, S. (2004).** Identification and characterization of Veph, a novel gene encoding a PH domain-containing protein expressed in the developing central nervous system of vertebrates. *Biochimie* **86**, 523–531.

**Nasevicius, A. & Ekker, S. C. (2000).** Effective targeted gene 'knockdown' in zebrafish. *Nat Genet* **26**, 216–220.

**Neuman, B. W., Stein, D. A., Kroeker, A. D., Paulino, A. D., Moulton, H. M., Iversen, P. L. & Buchmeier, M. J. (2004).** Antisense morpholino-oligomers directed against the 5′ end of the genome inhibit coronavirus proliferation and growth. *J Virol* **78**, 5891–5899.

**Panavas, T., Pogany, J. & Nagy, P. D. (2002).** Analysis of minimal promoter sequences for plus-strand synthesis by the *Cucumber necrosis virus* RNA-dependent RNA polymerase. *Virology* **296**, 263–274.

**Pasternak, A. O., van den Born, E., Spaan, W. J. M. & Snijder, E. J. (2001).** Sequence requirements for RNA strand transfer during nidovirus discontinuous subgenomic RNA synthesis. *EMBO J* **20**, 7220–7228.

**Pasternak, A. O., van den Born, E., Spaan, W. J. M. & Snijder, E. J. (2003).** The stability of the duplex between sense and antisense transcription-regulating sequences is a crucial factor in arterivirus subgenomic mRNA synthesis. *J Virol* **77**, 1175–1183.

**Pedersen, K. W., van der Meer, Y., Roos, N. & Snijder, E. J. (1999).** Open reading frame 1a-encoded subunits of the arterivirus replicase induce endoplasmic reticulum-derived double-membrane vesicles which carry the viral replication complex. *J Virol* **73**, 2016–2026.

**Peiris, J. S., Lai, S. T., Poon, L. L. & 13 other authors (2003).** Coronavirus as a possible cause of severe acute respiratory syndrome. *Lancet* **361**, 1319–1325.

**Saif, L. J., Redman, D. R., Brock, K. V., Kohler, E. M. & Heckert, R. A. (1988).** Winter dysentery in adult dairy cattle: detection of coronavirus in the faeces. *Vet Rec* **123**, 300–301.

**Sawicki, S. G. & Sawicki, D. L. (1995).** Coronaviruses use discontinuous extension for synthesis of subgenome-length negative strands. *Adv Exp Med Biol* **380**, 499–506.

**Snijder, E. J. & Meulenberg, J. J. M. (2001).** In *Fields Virology*, 4th edn, pp. 1205–1220. Edited by D. M. Knipe & P. M. Howley. Philadelphia, PA: Lippincott Williams & Wilkins.

**Summerton, J. (1999).** Morpholino antisense oligomers: the case for an RNase H-independent structural type. *Biochim Biophys Acta* **1489**, 141–158.

**Summerton, J. & Weller, D. (1997).** Morpholino antisense oligomers: design, preparation, and properties. *Antisense Nucleic Acid Drug Dev* **7**, 187–195.

**Tijms, M. A., van Dinten, L. C., Gorbalenya, A. E. & Snijder, E. J. (2001).** A zinc finger-containing papain-like protease couples subgenomic mRNA synthesis to genome translation in a positive-stranded RNA virus. *Proc Natl Acad Sci U S A* **98**, 1889–1894.

**Tortorici, M. A., Broering, T. J., Nibert, M. L. & Patton, J. T. (2003).** Template recognition and formation of initiation complexes by the replicase of a segmented double-stranded RNA virus. *J Biol Chem* **278**, 32673–32682.

**van den Born, E., Gultyaev, A. P. & Snijder, E. J. (2004).** Secondary structure and function of the 5′-proximal region of the equine arteritis virus RNA genome. *RNA* **10**, 424–437.

**van den Born, E., Posthuma, C. C., Gultyaev, A. P. & Snijder, E. J. (2005).** Discontinuous subgenomic RNA synthesis in arteriviruses is guided by an RNA hairpin structure located in the genomic leader region. *J Virol* **79**, 6312–6324.

**van Marle, G., Dobbe, J. C., Gultyaev, A. P., Luytjes, W., Spaan, W. J. M. & Snijder, E. J. (1999).** Arterivirus discontinuous mRNA transcription is guided by base pairing between sense and antisense transcription-regulating sequences. *Proc Natl Acad Sci U S A* **96**, 12056–12061.

**Zuniga, S., Sola, I., Alonso, S. & Enjuanes, L. (2004).** Sequence motifs involved in the regulation of discontinuous coronavirus subgenomic RNA synthesis. *J Virol* **78**, 980–994.